LIVER TRANSPLANTATION 21:442–453, 2015

ORIGINAL ARTICLE

Noninvasive 3-Dimensional Imaging of Liver Regeneration in a Mouse Model of Hereditary Tyrosinemia Type 1 Using the Sodium Iodide Symporter Gene

Raymond D. Hickey,[1,2] Shennen A. Mao,[2] Bruce Amiot,[2] Lukkana Suksanpaisan,[4] Amber Miller,[1] Rebecca Nace,[1] Jaime Glorioso,[2] Michael K. O'Connor,[3] Kah Whye Peng,[1] Yasuhiro Ikeda,[1] Stephen J. Russell,[1*] and Scott L. Nyberg[2*]

[1]*Departments of Molecular Medicine,* [2]*Surgery and,* [3]*Radiology, Mayo Clinic, Rochester, MN; and* [4]*Imanis Life Sciences, Rochester, MN*

Cell transplantation is a potential treatment for the many liver disorders that are currently only curable by organ transplantation. However, one of the major limitations of hepatocyte (HC) transplantation is an inability to monitor cells longitudinally after injection. We hypothesized that the thyroidal sodium iodide symporter (NIS) gene could be used to visualize transplanted HCs in a rodent model of inherited liver disease: hereditary tyrosinemia type 1. Wild-type C57Bl/6J mouse HCs were transduced ex vivo with a lentiviral vector containing the mouse *Slc5a5* (NIS) gene controlled by the thyroxine-binding globulin promoter. NIS-transduced cells could robustly concentrate radiolabeled iodine in vitro, with lentiviral transduction efficiencies greater than 80% achieved in the presence of dexamethasone. Next, NIS-transduced HCs were transplanted into congenic fumarylacetoacetate hydrolase knockout mice, and this resulted in the prevention of liver failure. NIS-transduced HCs were readily imaged in vivo by single-photon emission computed tomography, and this demonstrated for the first time noninvasive 3-dimensional imaging of regenerating tissue in individual animals over time. We also tested the efficacy of primary HC spheroids engrafted in the liver. With the NIS reporter, robust spheroid engraftment and survival could be detected longitudinally after direct parenchymal injection, and this thereby demonstrated a novel strategy for HC transplantation. This work is the first to demonstrate the efficacy of NIS imaging in the field of HC transplantation. We anticipate that NIS labeling will allow noninvasive and longitudinal identification of HCs and stem cells in future studies related to liver regeneration in small and large preclinical animal models. ***Liver Transpl 21:442-453, 2015***. © **2015 AASLD.**

Received August 26, 2014; accepted November 30, 2014.

Additional Supporting Information may be found in the online version of this article.

Abbreviations: 3-D, 3-dimensional; ALP, alkaline phosphatase; ALT, alanine aminotransferase; cDNA, complementary DNA; cPPT, central polyprimidine tract; CT, computed tomography; EDTA, ethylene diamine tetraacetic acid; EGF, epidermal growth factor; EGFP, enhanced green fluorescent protein; FAH, fumarylacetoacetate hydrolase; Fah–/–, fumarylacetoacetate hydrolase knockout; FBS, fetal bovine serum; GFP, green fluorescent protein; HBSS, Hanks' balanced salt solution; HC, hepatocyte; HEPES, 4-(2-hydroxyethyl)-1-piperazine ethanesulfonic acid; HT1, hereditary tyrosinemia type 1; LTR, long terminal repeat; LUT, lookup table; LV, lentiviral vector; MIP, maximum intensity images; MOI, multiplicity of infection; NIS, sodium iodide symporter; NTBC, 2-(2-nitro-4-trifluoromethylbenzyol)-1,3 cyclohexanedione; PET, positron emission tomography; RRE, rev-response element; SFFV, spleen focus forming virus; SPECT, single-photon emission computed tomography; TBG, thyroid hormone-binding globulin; TBIL, total bilirubin; Tx, transplantation; WPRE, woodchuck hepatitis virus posttranscription response element.

*Joint senior authors.

Contract grant sponsor: Center for Regenerative Medicine at Mayo Clinic, a National Institutes of Health T32 training grant; Contract grant number: DK007198.
Contract grant sponsor: Mayo Clinic Gary and Anita Klesch Predoctoral Fellowship and the Mayo Center for Clinical and Translational Science through the National Center for Advancing Translational Sciences; Contract grant number: UL1TR000135.

Address reprint requests to Raymond Hickey, Ph.D., Mayo Clinic, 200 First Street SW, Rochester, MN 55905. Telephone: 507-283-0878; FAX: 507-284-8388; E-mail: hickey.raymond@mayo.edu

DOI 10.1002/lt.24057
View this article online at wileyonlinelibrary.com.
LIVER TRANSPLANTATION.DOI 10.1002/lt. *Published on behalf of the American Association for the Study of Liver Diseases*

An alternative strategy to orthotopic liver transplantation is cell transplantation. A number of small animal models of metabolic liver diseases have been treated with hepatocyte (HC) transplantation. The first published partial correction of a metabolic disorder in humans was performed by Fox et al.[1] in a patient with Crigler-Najjar syndrome type 1. Since then, a number of patients with metabolic disorders have undergone HC transfusions with encouraging, albeit modest, success, as discussed in a previous work.[2] More recently, a number of alternative cell therapy strategies for liver disease, including the transplantation of pluripotent stem cells, liver stem cells, directly differentiated HC-like cells, and mesenchymal stem cells, have been attempted, as shown in previous studies.[3,4] One major limitation of current transplantation procedures is an inability to monitor cells noninvasively and longitudinally after infusion.[5] This current limitation is all the more important according to recent studies demonstrating extended periods of time, often up to 6 months, for complete differentiation of stem cells to occur in vivo.[6,7] Additionally, the ability of HCs to engraft and expand outside the liver[8,9] requires that an appropriate method be available to accurately identify the location of transplanted cells. Noninvasive, longitudinal molecular imaging, therefore, will play an essential part in not only identifying transplanted cells but also in helping to decipher the fate and differentiation of transplanted stem cells.

The thyroidal sodium iodide symporter (NIS) reporter gene (*Slc5a5*) is a promising candidate for this purpose, not only in preclinical animal model studies but also in clinical HC transplantation because this reporter has already been tested in other clinical human studies[10] and reviewed in a previous study.[11] NIS is an intrinsic plasma membrane glycoprotein that cotransports 2 sodium ions down the electrochemical gradient and 1 iodide ion up the electrochemical gradient from the plasma into the cell. NIS is normally expressed in thyroid follicular cells, stomach surface epithelium, and salivary gland ductal cells with minimal expression in the liver. Upon the addition of radiolabeled iodine (eg, I^{125}) or technetium-99m sodium pertechnetate (an iodide analogue) in vitro or in vivo, NIS-expressing cells can uptake the radiolabel, and this allows both qualitative and quantitative analyses of NIS-expressing cells by single-photon emission computed tomography (SPECT) or positron emission tomography (PET).[12] A key advantage to NIS imaging is that it is noninvasive and can be performed longitudinally to track HC engraftment, survival, and expansion.

In humans, hereditary tyrosinemia type 1 (HT1) is a severe, autosomal recessive inborn error of metabolism caused by a deficiency of fumarylacetoacetate hydrolase (FAH), a metabolic enzyme that catalyzes the last step of tyrosine metabolism.[13] Fumarylacetoacetate hydrolase knockout ($Fah^{-/-}$) mice have been used as a small animal model for HC transplantation.[14,15] In this model, engrafted FAH-positive cells have a selective growth advantage and can repopulate the $Fah^{-/-}$ liver in the absence of 2-(2-nitro-4-trifluoromethylbenzyol)-1,3 cyclohexanedione (NTBC). In the present study, we used $Fah^{-/-}$ mice to test the hypothesis that NIS-transduced HCs can be monitored noninvasively after transplantation with SPECT/computed tomography (CT) imaging to assess their repopulation in individual mice over time.

MATERIALS AND METHODS

Plasmid Construction

pSIN-CSGWdlNotl-based lentiviral vectors were produced from the parent vector pSIN-CSGWdlNotl–spleen focus forming virus (SFFV)–enhanced green fluorescent protein (EGFP), which contained the EGFP transgene controlled by the SFFV promoter.[16] Initially, the SFFV promoter was replaced with a construct that contained 2 copies of a human α1-microglobulin/bikunin enhancer and the promoter from the human thyroid hormone-binding globulin (TBG) gene.[17,18] Subsequently, the mouse *Slc5a5* complementary DNA (cDNA)[19] was cloned into the TBG vector in place of EGFP to produce the LV-TBG-NIS expression construct. In order to generate viral vectors, the LV-TBG-NIS expression construct, along with the packaging plasmid pCMVR8.91 and the vesicular stomatitis virus glycoprotein G–expressing plasmid, pMD.G,[20] were transiently transfected into 293 cells with Fugene6 (Roche, Indianapolis, IN). Transfected cells were washed after 16 hours and were grown for another 48 hours, after which supernatants were harvested and passed through a 0.45-μm filter. Vector supernatants were concentrated by ultracentrifugation (25,000 rpm, 1.5 hours at 4°C), and resuspended in serum-free media (OptiMEM, Life Technologies, Grand Island, CA), aliquoted, and stored at −80°C.

Animals and Animal Care

All animals received humane care in compliance with the regulations of the institutional animal care and use committee at Mayo Clinic. Donor C57Bl/6J mice (stock number 000664) were purchased from the Jackson Laboratories. Recipient $Fah^{-/-}$ mice[15] on the C57Bl/6J background were administered NTBC (Yecuris, Portland, OR) in the drinking water at 8 mg/L to prevent acute liver injury before transplantation.

Lentiviral Transduction Optimization

The lentiviral vector LV-SFFV-EGFP was transduced into primary mouse HCs at a multiplicity of infection (MOI) of 10. Media were changed every 2 days, and cells were analyzed for green fluorescent protein (GFP) expression by flow cytometry after 5 days. To dissociate cells into a single cell suspension, 0.05% tryspin/ethylene diamine tetraacetic acid (EDTA) was used. Cells were washed and fixed in 1% paraformaldehyde for 15 minutes before analysis on a FACSCalibur (BD

Biosciences, San Jose, CA). Data were analyzed with FlowJo (Treestar, Ashland, OR).

In Vitro Iodine Uptake Assay

The lentiviral vector LV-TBG-NIS was transduced into primary mouse HCs in a 12-well tissue culture plate at an MOI of 10. Media were changed every 2 days, and cells were assayed for the ability to uptake radiolabeled iodine after 5 days, as previously described.[21] Briefly, cells were washed with Hanks' balanced salt solution (HBSS; Sigma-Aldrich, St. Louis, MO) containing 10 mM 4-(2-hydroxyethyl)-1-piperazine ethanesulfonic acid (HEPES) and incubated with an activity of 1×105 cpm NaI (125I)/0.1 mL in 1 mL of HBSS containing HEPES. Also, 100 μM $KClO_4$ was added to inhibit NIS-mediated iodide influx in control wells. Plates were incubated at 37°C for 45 minutes. Cells were washed twice with ice-cold HBSS containing HEPES buffer. Cells were lysed with 1 M NaOH, and the activity was determined by γ-counting. All data points were measured in triplicate and displayed as means and standard errors of the mean.

SPECT/CT Imaging System

Imaging was performed in the Mayo Clinic Small Animal Imaging Core with a U-SPECT-II/CT scanner (MILabs, Utrecht, the Netherlands).[22] Animals were injected 1 hour before imaging by the intravenous administration of 0.5 mCi technetium-99m sodium pertechnetate diluted in 100 μL of saline. Scan volumes for both SPECT and CT were selected on the basis of orthogonal optical images provided by integrated webcams. Micro-CT image acquisition was performed in 4 minutes for normal resolution (169-μm square voxels, 640 slices) at 0.5 mA and 60 kV. The image acquisition time was approximately 20 minutes for SPECT (24 projections at 50 seconds per bed position). All pinholes focused on a single volume in the center of the tube, and with an XYZ stage, large volumes up to the entire animal could be scanned at uniform resolution.[23] Coregistration of the SPECT and CT images was performed by the application of precalibrated spatial transformation to the SPECT images to match the CT images. In order to mask background signals from the stomach, animals were administered 350 μL of undiluted barium sulfate (40% wt/vol; Tagitol V, E-Z-EM, Lake Success, NY) by oral gavage with a 22-gauge plastic feeding tube (Instech Laboratories, Plymouth, PA), as previously described.[24]

Image Reconstruction and Data Processing

SPECT reconstruction was performed with a pixel-based ordered subset expectation maximization algorithm[25] with 6 iterations and 16 subsets. CT data were reconstructed with a Feldkamp cone beam algorithm (NRecon v1.6.3, Skyscan). After reconstruction, SPECT images were automatically registered to the CT images according to the precalibrated transformation, and they were resampled to the CT voxel size. Coregistered images were further rendered and visualized with PMOD software (PMOD Technologies, Zurich, Switzerland). A 3-dimensional (3-D) Gaussian filter (0.8-mm full width at half maximum) was applied to suppress noise, and LUTs were adjusted for good visual contrast. Reconstructed images were visualized as both orthogonal slices and maximum-intensity projections. Maximal-intensity-projection videos and 3-D rendering of regions of interests were performed with the PMOD software.

Histology and Biochemical Analysis

For histology analysis, tissue samples were fixed in 10% neutral buffered formalin (Protocol, Fisher-Scientific, Pittsburgh, PA) and processed for paraffin embedding and sectioning. For hematoxylin and eosin staining, slides were prepared with standard protocols. FAH immunohistochemistry using a polyclonal rabbit anti-FAH primary antibody[26] was performed with a Bond III automatic stainer (Leica, Buffalo Grove, IL) with a 20-minute antigen retrieval step using Bond Epitope Retrieval Solution 2 (Leica, Buffalo Grove, IL), and it was stained with diaminobenzidine (Leica, Buffalo Grove, IL). For biochemical analysis of alkaline phosphatase (ALP), alanine aminotransferase (ALT), and total bilirubin (TBIL), plasma was analyzed with the VetScan VS2 benchtop analyzer (Mammalian Liver Profile, Abaxis, Union City, CA) according to the manufacturer's instructions.

HC Transplantation

HCs were harvested with a typical 2-step collagenase perfusion technique, as described in a previous work.[27] The number and viability of cells were determined by trypan blue exclusion. Also, 0.5×10^6 cells were plated into 6-well Primaria culture plates (BD Biosciences, San Jose, CA) containing the following media: Dulbecco's modified Eagle's medium (Thermo Fisher Scientific, Waltham, MA), 10% heat-inactivated fetal bovine serum (FBS; Corning, Herndon, VA), 10 mM HEPES (Corning, Herndon, VA), and penicillin/streptomycin (Corning, Herndon, VA). Fresh media were replaced 2 hours later, and they contained 10 μM dexamethasone (Sigma-Aldrich, St. Louis, MO) and 10 ng/mL epidermal growth factor (EGF; Sigma-Aldrich, St. Louis, MO). Lentiviral vectors were added to the media at a multiplicity of infection that was determined with p24 enzyme-linked immunosorbent assay (Clontech, Mountain View, CA). HCs were harvested the following day with 0.05% tryspin/EDTA (Corning, Herndon, VA). The number and viability of cells were determined by trypan blue exclusion. HCs were resuspended in a volume of growth media (100 μL) containing 2 μg/mL DNaseI (Sigma-Aldrich, St. Louis, MO) to minimize the clumping of cells. Cells were injected via the spleen with standard intrasplenic injection protocols.[28]

Primary HC Spheroids

Freshly isolated HCs were suspended in Williams E medium supplemented with 10% FBS, 10 U/mL penicillin G, 100 μg/mL streptomycin, 10 μg/mL insulin, 5.5 μg/mL transferrin, and 5 ng/mL sodium selenite at a concentration of 1×10^6 viable cells/mL. HC suspensions of 20 mL were inoculated into spheroid dishes ($10 \times 8 \times 2$ cm^3) custom-made with glass and siliconized with Sigmacote. Spheroid dishes were placed in the 37°C incubator with 5% CO_2 and rocked continuously at 10 cycles per minute for 48 hours to induce spheroid formation.

RESULTS

Lentiviral-Mediated Transgene Expression is Increased in the Presence of Dexamethasone

In future clinical studies, efficient ex vivo HC transduction protocols will be required in order for ex vivo HC gene therapy to be successful.[29,30] Rodent HCs in particular are resistant to lentiviral transduction, with transduction efficiencies < 50% commonly reported. However, recent progress has been made by the inclusion of growth factors such as EGF in transduction media, which have allowed higher transduction efficiencies to be achieved.[31] We initially tested the effect of EGF on lentiviral transduction with a lentiviral vector expressing EGFP controlled by the ubiquitous SFFV promoter, but we did not detect a significant difference in EGFP-positive cells that contained EGF in the transduction media (Fig. 1A and Supporting Fig. 1). Next, we added dexamethasone to the media and noticed a significant increase in EGFP-positive cells, which was independent of EGF. On the basis of these results, lentiviral transduction of primary HCs was performed in the presence of dexamethasone and EGF for the remaining experiments.

NIS-Transduced Mouse HCs Can Concentrate Radiolabeled Iodine In Vitro

It is unknown whether HCs have the ability to concentrate iodine if NIS is exogenously expressed. With our optimized transduction protocol, primary HCs were transduced with a lentiviral vector expressing NIS controlled by a liver-specific promoter (LV-TBG-NIS; see the Materials and Methods section for details). HCs were cultured for 5 days, after which the ability of these cells to take up iodine intracellularly was assessed with I-125 (Fig. 1B). NIS-transduced HCs had significantly increased uptake of radioisotope in comparison with nontransduced HCs when I-125 was added to the media for 45 minutes. Importantly, the ability of NIS-transduced HCs to concentrate the radioisotope was significantly abrogated by the addition of the NIS-competitive inhibitor potassium perchlorate in the media; this indicated that the expression of NIS was responsible for increased radioisotope uptake in transduced HCs.

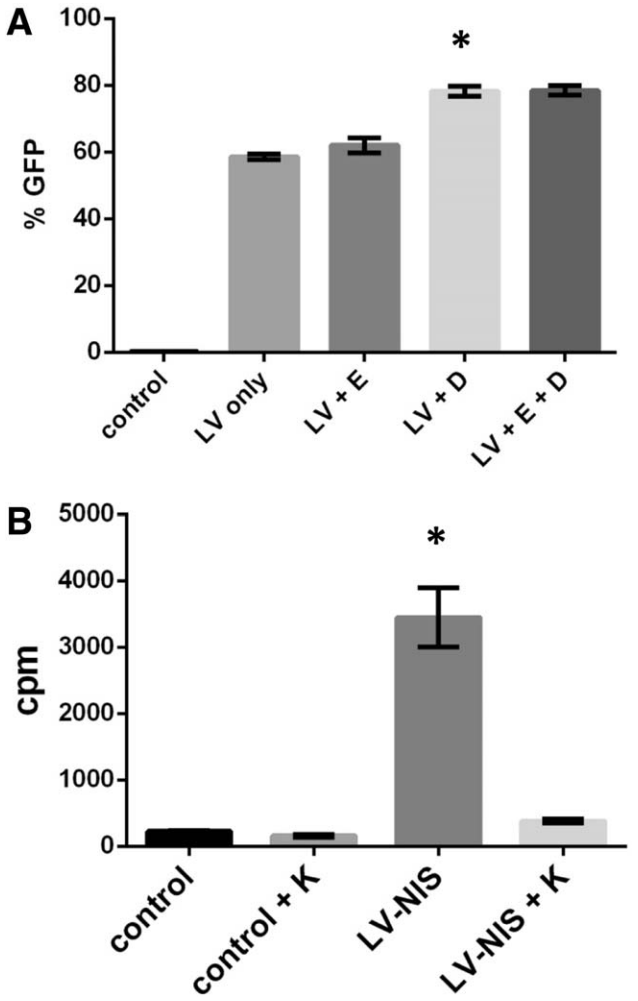

Figure 1. Ex vivo transduction of primary HCs. (A) Quantification of flow cytometry data based on GFP expression after lentiviral vector transduction of HCs with LV-TBG-GFP with or without the addition of EGF (E) and dexamethasone (D). *$P < 0.01$. (B) In vitro radiolabeled iodine (I-125) uptake assay showing a significant increase in I-125 uptake in LV-TBG-NIS transduced HCs. I-125 uptake in LV-TBG-NIS transduced HCs was blocked with the addition of potassium perchlorate (K). *$P < 0.01$.

NIS-Transduced Mouse HCs Can Concentrate Radionuclides In Vivo

Transplanted FAH-positive HCs have a selective growth advantage over resident Fah$^{-/-}$ HCs when mice are taken off the protective drug NTBC.[32] As a pilot experiment, primary HCs from FAH-positive wild-type mice were isolated and labeled with LV-TBG-NIS before transplantation into Fah$^{-/-}$ mice (Fig. 2). As a control, non-NIS labeled HCs were also transplanted into Fah$^{-/-}$ mice. Mice underwent NTBC withdrawal and selection, and SPECT/CT imaging using technetium-99m sodium pertechnetate was performed after 12 weeks. In a control animal transplanted with HCs not labeled with NIS, isotope uptake was not detected in the liver (Fig. 3A and Supporting Video 1). In contrast, in mice transplanted with NIS-transduced HCs, robust uptake of the isotope was visible in the liver of these animals, and this confirmed repopulation

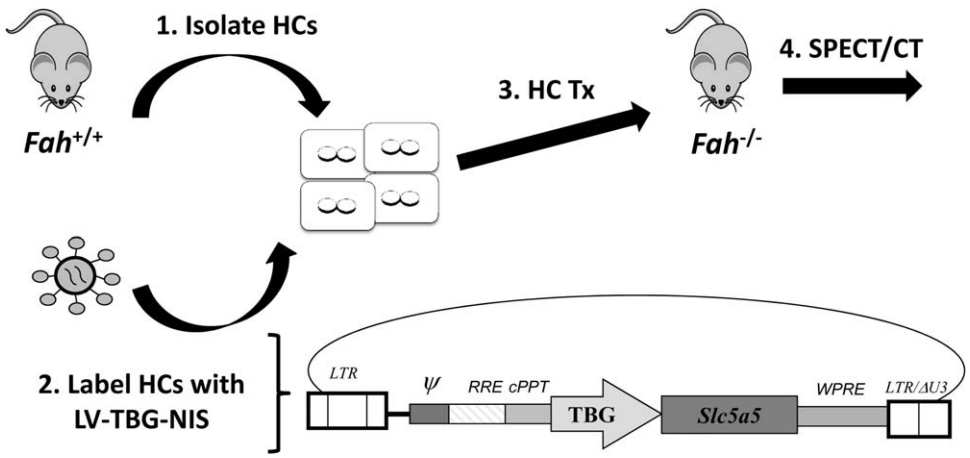

Figure 2. Summary of the in vivo HC transplantation procedure. HCs were transduced with a lentiviral vector expressing NIS before Tx. A schematic of the vector is also included that contained the NIS gene (*Slc5a5*).

of the host liver with NIS-transduced cells (Fig. 3A,B and Supporting Video 2). Finally, SPECT imaging indicated that repopulation of the liver by donor HCs was not uniform (Fig. 3B). In order to confirm this histologically, FAH-immunohistochemistry was performed. Consistent with the imaging data, transplanted cells were detected nonuniformly throughout the liver (Fig. 3C).

NIS-Imaging Permits Longitudinal 3-D Imaging of Repopulating HCs in Fah$^{-/-}$ Livers

We next set out to determine whether SPECT/CT imaging could be used to quantitatively monitor repopulation kinetics longitudinally in individual mice. Mice underwent transplantation intrasplenically with 5×10^4 HCs labeled with LV-TBG-NIS. Animals underwent NTBC selection, and SPECT/CT imaging using technetium-99m sodium pertechnetate (half-life of 6 hours) was performed at 2 different time points: after 41 and 85 days of NTBC selection. In this group of 4 mice (numbered 160.01, 160.10, 160.20, and 160.30), there was a statistically significant increase in radiolabel uptake during the 2 time points (Fig. 4A), and this is consistent with previous data that FAH-positive cells can expand in the Fah$^{-/-}$ liver. Additionally, this increase in liver uptake could be directly visualized at the 2 time points, and this

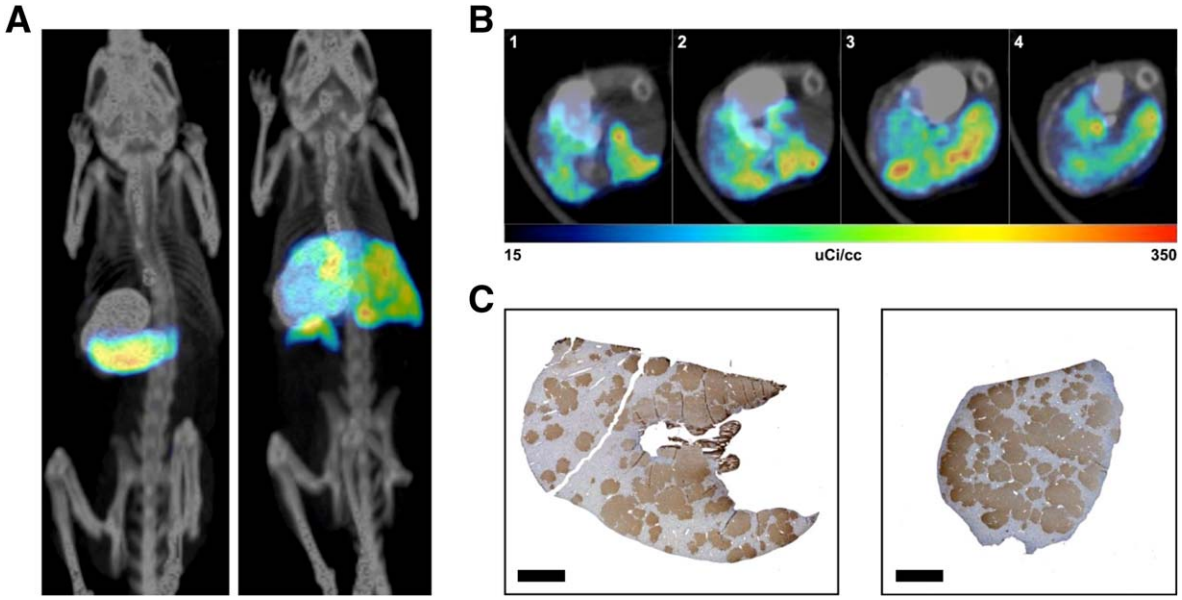

Figure 3. In vivo imaging of NIS-transduced HCs after 12 weeks of NTBC selection. (A) Representative fused MIP of control HC-injected (left) and NIS-transduced HC-injected (right) mice. The location of the stomach was identified by the oral administration of barium sulfate before imaging. The signals from the thyroid and bladder were removed from both animals. Radionuclide-uptake was still visible in the lower stomach of the control mouse. The relative intensity of radioisotope uptake is represented as low (colored blue) to high (colored red). (B) Representative transverse SPECT/CT sections of an NIS-transduced HC-transplanted liver, showing different positions of the liver from the head (1) to feet (4) of the animal. (C) FAH-immunohistochemistry of the same liver showing nonuniform distribution of transplanted cells in 2 different lobes from the same mouse. FAH-positive cells are stained brown. The scale bar represents 2 mm.

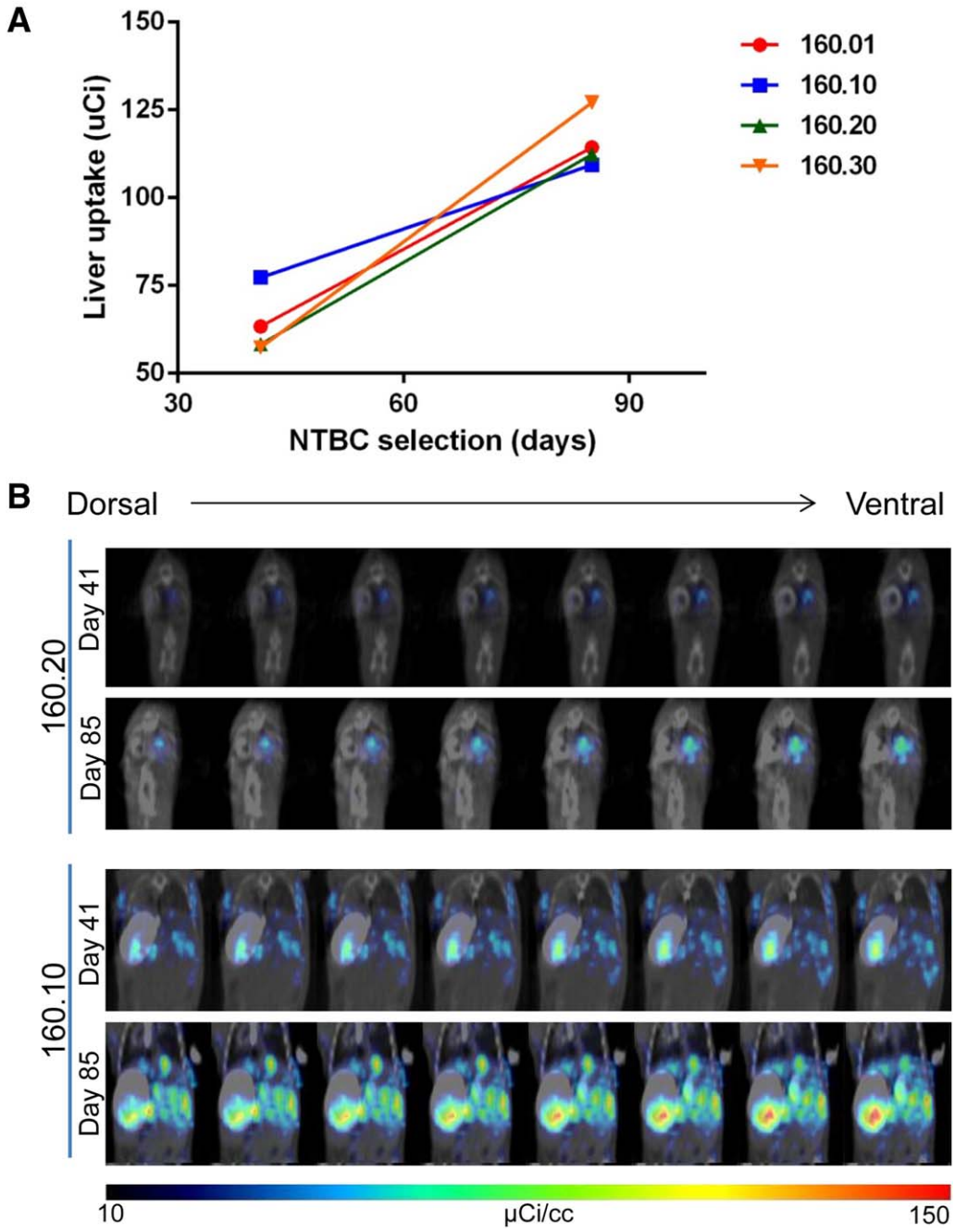

Figure 4. Longitudinal imaging of individual transplanted mice. (A) Quantification of liver uptake of technetium-99m sodium pertechnetate in 4 mice transplanted with NIS-transduced cells. Mice were imaged after 41 and 85 days of NTBC selection. (B) Representative images from 2 mice (160.10 and 160.20) showing an increase in technetium-99m sodium pertechnetate uptake in the liver over time. Eight serial sections through similar locations at the 2 time points were used to demonstrate the regeneration of individual cell clusters over time.

revealed expansion of individual cell clusters over time throughout the livers of single animals (Fig. 4B). The general shape and location of nodules were consistent over time, but size and uptake intensity increased; this indicated the expansion of cells.

Furthermore, SPECT/CT imaging was able to resolve individual nodules of transplanted cells. An analysis of serial SPECT/CT sections demonstrated distinct nodules increasing and then decreasing in nodule diameter and uptake intensity, and this revealed that individual nodule geometry is most similar to spherical geometry (Fig. 5).

NIS-Labeling of HCs Does Not Affect HC Function In Vivo

Because NIS is not normally expressed in the liver, we asked whether forced expression of NIS in HCs would

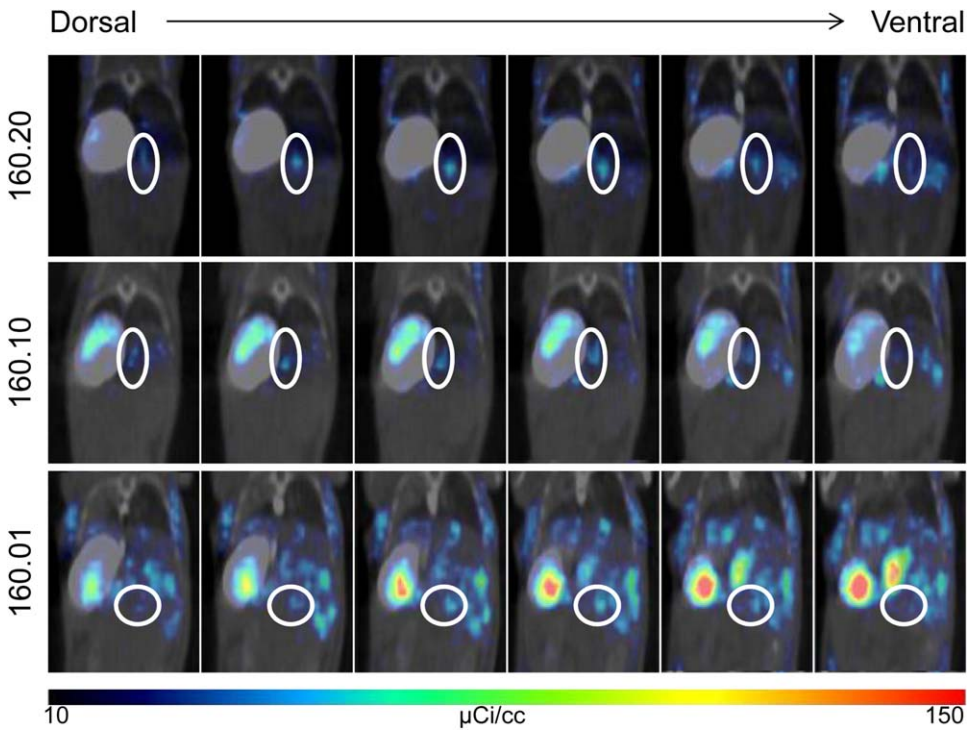

Figure 5. High-resolution imaging of individual regenerating nodules. Near-serial SPECT/CT sections through individual nodules in 3 separate mice show increasing and then decreasing nodule diameter and uptake at day 41 of NTBC selection. White ovals highlight the individual nodule being followed. The location of the stomach was identified by oral administration of barium sulfate before imaging.

negatively affect liver function in transplanted mice. In the absence of transplanted HCs, $Fah^{-/-}$ mice die of acute liver failure when the protective drug NTBC is removed from their drinking water.[15,33] Transplantation and expansion of NIS-transduced HCs (Fig. 4) did not negatively affect the rescue of liver failure in $Fah^{-/-}$ mice. After NTBC withdrawal, mice survived long term and continued to gain weight over time in comparison with nontransplanted controls (data not shown). Histologically, the livers of transplanted mice appeared normal, and in contrast to $Fah^{-/-}$ mice off NTBC, there was no evidence of the profound HC damage typically seen in $Fah^{-/-}$ mice off NTBC (Fig. 6A-C). Consistent with the histological data, a biochemical analysis of plasma indicated no significant liver damage in NIS-transduced HC-transplanted mice (Fig. 6D-F). Similar to $Fah^{-/-}$ mice on NTBC, transplanted mice had significantly reduced levels of ALP, ALT, and TBIL in comparison with $Fah^{-/-}$ mice off NTBC.

NIS-Labeling Enables Noninvasive Imaging of HC Spheroid Engraftment In Vivo

It has been previously demonstrated that primary HC spheroids can be formed with a rocking suspension technique.[34,35] Although cultures of HCs as spheroids have been shown to maintain cellular function better than other in vitro culture methods,[36] engraftment has not been demonstrated in a mouse model of metabolic disease. We initially tested whether pig HCs could be transduced by lentiviral vectors during spheroid formation with vectors expressing either GFP (LV-TBG-GFP) or NIS (LV-TBG-NIS) controlled by the TBG promoter. Robust GFP-positive expression could be detected in LV-TBG-GFP transduced cells after formed spheroids were plated as a monolayer (Fig. 7A). Additionally, LV-TBG-NIS-transduced cells were able to uptake radiolabeled iodine in vitro (Fig. 7B). Next, wild-type mouse HCs from a C57Bl6/6J donor were rocked in vitro for 48 hours in the presence of LV-TBG-NIS. HC spheroids were formed that had an average diameter of 60 μm. These spheroids were injected directly into the liver parenchyma of recipient $Fah^{-/-}$ mice, and SPECT/CT imaging was used to identify and monitor cells longitudinally. Mice were imaged 13 and 28 days after transplantation, and this revealed a consistent and specific focus of radiolabel uptake at the site of injection (Fig. 7C and Supporting Fig. 2A). Subsequently, FAH-immunohistochemistry was performed to confirm the detection of donor cells, and this revealed that FAH-positive transplanted spheroids had integrated normally into the parenchyma of the $Fah^{-/-}$ liver (Fig. 7D and Supporting Fig. 2B).

DISCUSSION

In the current study, we tested the ability of the NIS reporter gene to be used to monitor HC repopulation in a mouse model of HT1 with SPECT/CT imaging. In

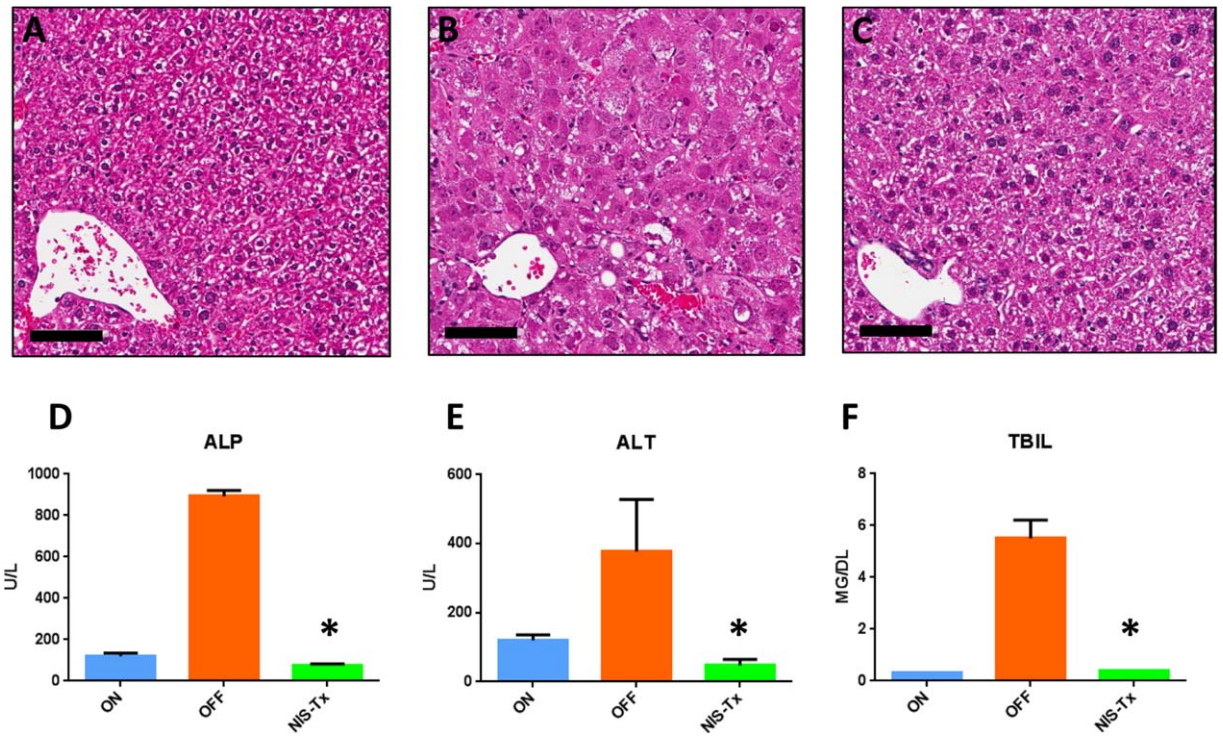

Figure 6. NIS labeling does not affect HC biology. Representative images of H&E stained livers of $Fah^{-/-}$ mice (A) on NTBC, (B) off NTBC for 25 days, and (C) 85 days after repopulation with NIS-transduced HCs. The scale bar represents 80 μm. (D-F) Biochemical analysis of levels of plasma ALP, ALT, and TBIL of $Fah^{-/-}$ mice on NTBC (left), off NTBC (middle), and after repopulation with NIS-transduced HCs (right). *$P < 0.01$.

order to label HCs with the reporter gene, we used a lentiviral vector expressing NIS that was controlled by a liver-specific promoter to permanently label the cells through lentiviral-mediated integration of the transgene. Labeled HCs were transplanted by intrasplenic injection, and SPECT/CT imaging was performed longitudinally to quantitatively and qualitatively assess HC repopulation. Repopulation kinetics appeared similar to those previously published with the $Fah^{-/-}$ mouse,[26] in which repopulation of the donor liver occurs rapidly by replication and expansion of the transplanted FAH-positive cells. Additionally, NIS-labeling appeared to not have any negative effect on HC biology, and repopulated mice were rescued from acute liver failure caused by FAH deficiency.[33]

A number of imaging modalities, including fluorescence imaging, bioluminescence imaging, SPECT, PET, and magnetic resonance imaging, have been used to visualize cells in vivo as previously reviewed.[37] The most common method for imaging cells in a small animal is the use of the luciferase reporter gene for bioluminescence imaging.[38] Although this method has been shown to label various cell types in vivo, including HCs,[9,39] its more widespread use is limited by a number of critical factors, including limited resolution, elicitation of an immune response against the foreign transgene, and an inability to image fluorescence in deep tissue (>2 cm), which is particularly relevant to the liver.[40,41] As better preclinical large animal models become available,[42-44] the ability to perform noninvasive in vivo imaging will be critical for several aspects of regenerative medicine, including gene therapy and cell therapy. Therefore, although luciferase imaging will continue to be an acceptable modality for in vivo imaging in small animals, alternative in vivo imaging protocols will be required for preclinical studies in larger animals. An alternative strategy is to label HCs before transplantation with a radionuclide, such as the inert metal indium-111 (^{111}In)-oxine. With this method, it has been demonstrated that HCs can incorporate ^{111}In, and this allows in vivo SPECT imaging to identify the biodistribution of transplanted cells.[45,46] Initial studies in mice and rats have now been replicated in human studies.[47,48] However, although this method clearly demonstrates the efficacy and safety of SPECT imaging with a radionuclide, it is limited by 3 key factors: only short-term imaging is possible because the radiolabel is lost within days, HC labeling efficiencies are low, and the detection of ^{111}In is independent of cell viability.

The NIS reporter has a number of advantages for noninvasive imaging of transplanted cells. First, no immune response was apparent in these studies on the basis of long-term detection of NIS-positive cells, and this confirms previous reports of nonimmunogenicity with this reporter gene and is consistent with the fact that NIS is normally expressed in several cell types in the body, including the thyroid and stomach.[11] Second, the NIS cDNA is small enough (<3-kb

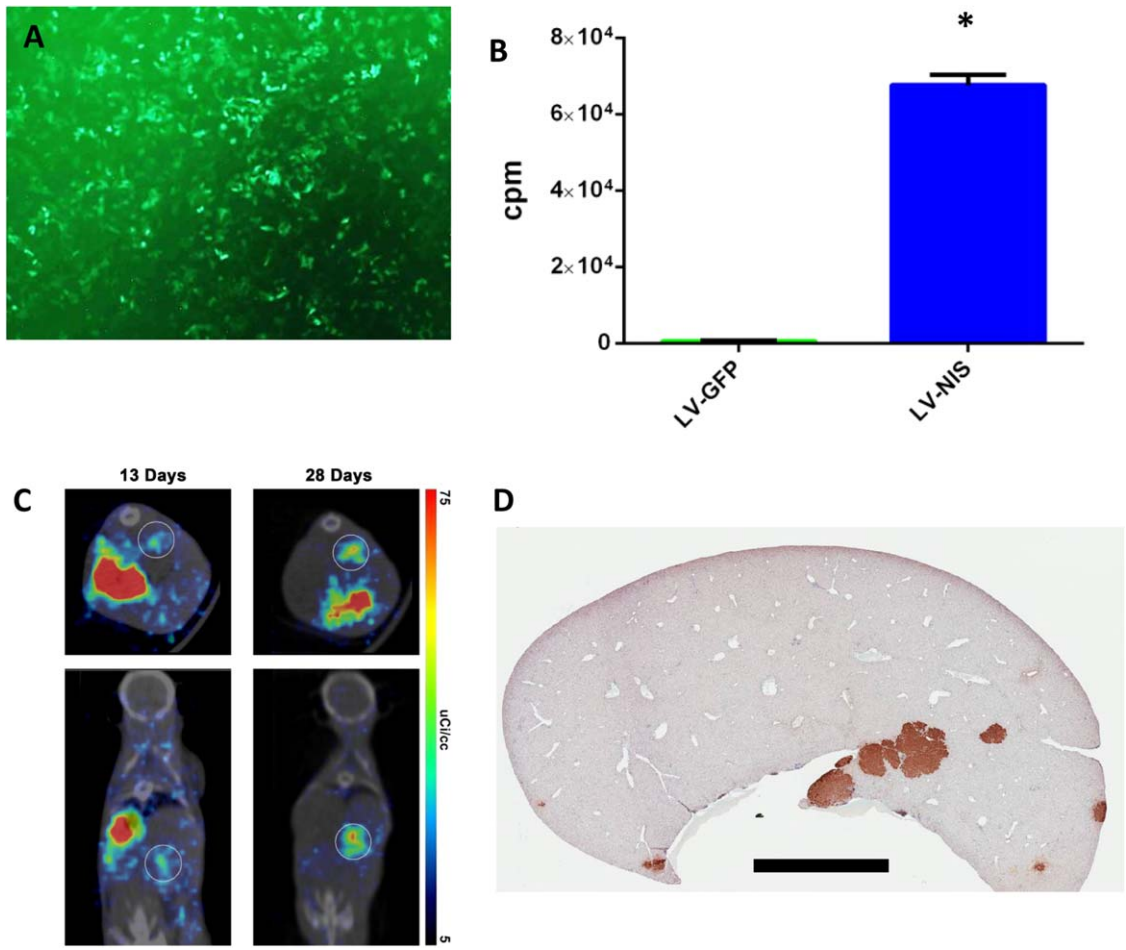

Figure 7. HC spheroids can engraft in vivo. (A) Detection of GFP-positive cells in vitro after transduction of HCs during rocked spheroid formation. (B) In vitro radiolabeled iodine (I-125) uptake assay showing a significant increase in LV-TBG-NIS transduced spheroids versus control LV-TBG-GFP transduced spheroids. *$P < 0.01$. (C) Representative images after 13 (left) and 28 days (right) of a single mouse injected with NIS-transduced spheroids. In the right image, the signal from the stomach was masked with barium sulfate administration. (D) FAH-immunohistochemistry of the same liver showing donor FAH-positive cells (stained brown) integrated in the liver parenchyma. The scale bar represents 2 mm.

messenger RNA) that in addition to its use in lentiviral vectors, NIS has the ability to be cloned into various vectors, including those with small packaging capacities such as adeno-associated virus. Third, SPECT and PET imaging will be necessary for deep tissue penetration to detect transplanted cells in preclinical models, such as pigs,[49] as well as human clinical trials.[10] This is a critical disadvantage of luciferase reporter imaging that is unlikely to be overcome. Fourth, SPECT imaging can be performed longitudinally for months and potentially years when cells are labeled with an integrated gene such as NIS. This is in contrast to ^{111}In labeling, which is a useful parameter for monitoring the short-term biodistribution of cells but cannot be used for long-term studies.[48] Fifth, although it was not possible to directly compare luciferase and SPECT imaging directly in these experiments, the resolution at which SPECT/CT could identify individual nodules of FAH-positive cells was superior to any previously published data that used luciferase for HC imaging.[50,51] Finally, NIS could be used as a suicide gene to provide an additional safety mechanism for clinical cell therapies. To date, genes such as herpesvirus thymidine kinase[52] and iCasp9[53] have been used; however, those genes can be immunogenic and can induce undesired immune responses upon cell transplantation. In contrast, the NIS gene facilitates arming with a nonimmunogenic suicide mechanism upon treatment with I^{131}. Using NIS as a reporter, we were able to demonstrate for the first time engraftment and survival of primary HC spheroids after a direct injection into the parenchyma. Since the initial preclinical experiments in a rodent model for Crigler-Najjar syndrome type 1, a number of small animal models of metabolic liver diseases have been treated by HC transplantation.[32,54,55] These animal experiments have paved the way for a number of human HC transplants to occur, including the first published partial correction in a patient with metabolic liver disease in 1998.[1,5] However, one of the primary limitations of HC transplantation is the low efficiency of cell engraftment. Different strategies, including conditioning of the donor liver[56] and grafting of cells embedded in biomaterials,[39] have been

proposed to improve engraftment. It has been previously demonstrated that rat HC spheroids formed by a rocked technique maintain differentiated HC gene expression and function.[36] The data presented here build upon those studies by demonstrating a potential new strategy for HC transplantation. Additionally, maintenance of HC function in vitro will be a critical component for ongoing ex vivo gene correction strategies. Therefore, the culture of HCs as spheroids may provide a novel resource for future gene therapy protocols.

On the basis of the data presented here, we believe that the NIS reporter could be used in future clinical cell transplantation protocols, particularly in the case of ex vivo gene therapy for metabolic liver disease.[29,30] The efficacy and safety of ex vivo gene addition have been demonstrated in the hematopoietic field, in which a number of patients have undergone successful gene therapy with lentiviral vectors.[57,58] We predict the evolution of similar protocols for treating metabolic liver disease. Consequently, because these protocols already require the integration of a functional gene with a lentiviral vector, the addition of a reporter gene to these constructs should not affect their safety or efficacy, as has been shown previously in other mouse models of liver disease.[59,60] Nonetheless, there are safety aspects related to the use of radionuclides and nuclear imaging that would need to be considered before the introduction of the NIS reporter into the clinic for metabolic liver disease gene therapy. One concern with this technique is the potential DNA damage caused by the injected radionuclide. Although the use of I-125 would not be considered a suitable tracer for imaging patients because of the significant radiation dose associated with its use, technetium-99m sodium pertechnetate delivers an effective radiation dose that is 100 times lower than that of I-125. Furthermore, studies have shown that technetium-99m in the form of sodium pertechnetate appears to have a low potential to induce DNA damage in cells.[61] This fact, combined with the low effective dose from this radiotracer, makes it an ideal candidate imaging agent for serial studies in combination with the NIS reporter. Another potential concern with repeated SPECT/CT imaging in these patients is the cumulative radiation exposure over time and the associated risks of radiation-induced cancer. A single SPECT study typically requires the administration of ~5 mCi of technetium-99m sodium pertechnetate and delivers an effective radiation dose of ~2.4 mSv,[62] although the typical low-dose CT scan used for anatomical correlation delivers an additional 1.5 mSv.[63] The combined dose of 3.5 mSv is comparable to the average background radiation level of 3.1 mSv in the United States.[64] At these low doses, hypothetical risk estimates of cancer are not recommended because of an absence of radiation-specific biomarkers for health effects and the failure of epidemiological studies to demonstrate any risk.[65]

In conclusion, we were able to monitor for the first time the fate of transplanted HCs in a small animal model of metabolic disease with noninvasive 3-D imaging. NIS-transduced HCs allowed high-resolution imaging of individual clusters of cells, and these cells could be longitudinally monitored in individual animals with the simple and safe imaging modality SPECT. Importantly, NIS imaging had no apparent impact on HC function or replication capacity, and this implies that it has the potential to be an ideal candidate reporter for future clinical HC transplantations.

ACKNOWLEDGMENT

RDH was funded by an American Liver Foundation Postdoctoral Fellowship Award. We thank Markus Grompe (Oregon Health and Science University, Portland, OR) for generously providing $Fah^{-/-}$ mice for use in this study. Funding for importing mice was provided by the Center for Cell Signaling in Gastroenterology at Mayo Clinic. We thank LouAnn Gross (Mayo Clinic, Rochester, MN) and Jenny Pattengill (Mayo Clinic, Scottsdale, AZ) for histology support and Tracy Decklever and Dianna Glynn (Mayo Clinic, Rochester, MN) for SPECT/CT imaging.

REFERENCES

1. Fox IJ, Chowdhury JR, Kaufman SS, Goertzen TC, Chowdhury NR, Warkentin PI, et al. Treatment of the Crigler-Najjar syndrome type I with hepatocyte transplantation. N Engl J Med 1998;338:1422-1426.
2. Dhawan A, Puppi J, Hughes RD, Mitry RR. Human hepatocyte transplantation: current experience and future challenges. Nat Rev Gastroenterol Hepatol 2010;7:288-298.
3. Huebert RC, Rakela J. Cellular therapy for liver disease. Mayo Clin Proc 2014;89:414-424.
4. Yu Y, Fisher JE, Lillegard JB, Rodysill B, Amiot B, Nyberg SL. Cell therapies for liver diseases. Liver Transpl 2012;18:9-21.
5. Hughes RD, Mitry RR, Dhawan A. Current status of hepatocyte transplantation. Transplantation 2012;93: 342-347.
6. Kroon E, Martinson LA, Kadoya K, Bang AG, Kelly OG, Eliazer S, et al. Pancreatic endoderm derived from human embryonic stem cells generates glucose-responsive insulin-secreting cells in vivo. Nat Biotechnol 2008;26:443-452.
7. Zhu S, Rezvani M, Harbell J, Mattis AN, Wolfe AR, Benet LZ, et al. Mouse liver repopulation with hepatocytes generated from human fibroblasts. Nature 2014;508:93-97.
8. Hoppo T, Komori J, Manohar R, Stolz DB, Lagasse E. Rescue of lethal hepatic failure by hepatized lymph nodes in mice. Gastroenterology 2011;140:656-666.
9. Komori J, Boone L, DeWard A, Hoppo T, Lagasse E. The mouse lymph node as an ectopic transplantation site for multiple tissues. Nat Biotechnol 2012;30:976-983.
10. Russell SJ, Federspiel MJ, Peng KW, Tong C, Dingli D, Morice WG, et al. Remission of disseminated cancer after systemic oncolytic virotherapy. Mayo Clin Proc 2014;89: 926-933.
11. Penheiter AR, Russell SJ, Carlson SK. The sodium iodide symporter (NIS) as an imaging reporter for gene, viral, and cell-based therapies. Curr Gene Ther 2012;12:33-47.
12. Cho JY. A transporter gene (sodium iodide symporter) for dual purposes in gene therapy: imaging and therapy. Curr Gene Ther 2002;2:393-402.

13. Lindblad B, Lindstedt S, Steen G. On the enzymic defects in hereditary tyrosinemia. Proc Natl Acad Sci U S A 1977;74:4641-4645.
14. Overturf K, al-Dhalimy M, Ou CN, Finegold M, Grompe M. Serial transplantation reveals the stem-cell-like regenerative potential of adult mouse hepatocytes. Am J Pathol 1997;151:1273-1280.
15. Grompe M, al-Dhalimy M, Finegold M, Ou CN, Burlingame T, Kennaway NG, Soriano P. Loss of fumarylacetoacetate hydrolase is responsible for the neonatal hepatic dysfunction phenotype of lethal albino mice. Genes Dev 1993;7:2298-2307.
16. Nelson TJ, Martinez-Fernandez A, Yamada S, Mael AA, Terzic A, Ikeda Y. Induced pluripotent reprogramming from promiscuous human stemness related factors. Clin Transl Sci 2009;2:118-126.
17. Harding CO, Gillingham MB, Hamman K, Clark H, Goebel-Daghighi E, Bird A, Koeberl DD. Complete correction of hyperphenylalaninemia following liver-directed, recombinant AAV2/8 vector-mediated gene therapy in murine phenylketonuria. Gene Ther 2006;13:457-462.
18. Wang L, Takabe K, Bidlingmaier SM, Ill CR, Verma IM. Sustained correction of bleeding disorder in hemophilia B mice by gene therapy. Proc Natl Acad Sci U S A 1999; 96:3906-3910.
19. Pinke LA, Dean DS, Bergert ER, Spitzweg C, Dutton CM, Morris JC. Cloning of the mouse sodium iodide symporter. Thyroid 2001;11:935-939.
20. Zufferey R, Nagy D, Mandel RJ, Naldini L, Trono D. Multiply attenuated lentiviral vector achieves efficient gene delivery in vivo. Nat Biotechnol 1997;15:871-875.
21. Dingli D, Peng KW, Harvey ME, Greipp PR, O'Connor MK, Cattaneo R, et al. Image-guided radiovirotherapy for multiple myeloma using a recombinant measles virus expressing the thyroidal sodium iodide symporter. Blood 2004;103:1641-1646.
22. van der Have F, Vastenhouw B, Ramakers RM, Branderhorst W, Krah JO, Ji C, et al. U-SPECT-II: An ultra-high-resolution device for molecular small-animal imaging. J Nucl Med 2009;50:599-605.
23. Vastenhouw B, Beekman F. Submillimeter total-body murine imaging with U-SPECT-I. J Nucl Med 2007;48: 487-493.
24. Suksanpaisan L, Pham L, McIvor S, Russell SJ, Peng KW. Oral contrast enhances the resolution of in-life NIS reporter gene imaging. Cancer Gene Ther 2013;20:638-641.
25. Branderhorst W, Vastenhouw B, Beekman FJ. Pixel-based subsets for rapid multi-pinhole SPECT reconstruction. Phys Med Biol 2010;55:2023-2034.
26. Wang X, Montini E, Al-Dhalimy M, Lagasse E, Finegold M, Grompe M. Kinetics of liver repopulation after bone marrow transplantation. Am J Pathol 2002;161:565-574.
27. Grompe M, Jones SN, Loulseged H, Caskey CT. Retroviral-mediated gene transfer of human ornithine transcarbamylase into primary hepatocytes of spf and spf-ash mice. Hum Gene Ther 1992;3:35-44.
28. Ponder KP, Gupta S, Leland F, Darlington G, Finegold M, DeMayo J, et al. Mouse hepatocytes migrate to liver parenchyma and function indefinitely after intrasplenic transplantation. Proc Natl Acad Sci U S A 1991;88:1217-1221.
29. Grossman M, Raper SE, Kozarsky K, Stein EA, Engelhardt JF, Muller D, et al. Successful ex vivo gene therapy directed to liver in a patient with familial hypercholesterolaemia. Nat Genet 1994;6:335-341.
30. Grossman M, Rader DJ, Muller DW, Kolansky DM, Kozarsky K, Clark BJ, 3rd, et al. A pilot study of ex vivo gene therapy for homozygous familial hypercholesterolaemia. Nat Med 1995;1:1148-1154.
31. Rothe M, Rittelmeyer I, Iken M, Rüdrich U, Schambach A, Glage S, et al. Epidermal growth factor improves lentivirus vector gene transfer into primary mouse hepatocytes. Gene Ther 2012;19:425-434.
32. Overturf K, Al-Dhalimy M, Tanguay R, Brantly M, Ou CN, Finegold M, Grompe M. Hepatocytes corrected by gene therapy are selected in vivo in a murine model of hereditary tyrosinaemia type I. Nat Genet 1996;12:266-273.
33. Grompe M, Lindstedt S, al-Dhalimy M, Kennaway NG, Papaconstantinou J, Torres-Ramos CA, et al. Pharmacological correction of neonatal lethal hepatic dysfunction in a murine model of hereditary tyrosinaemia type I. Nat Genet 1995;10:453-460.
34. Nyberg SL, Hardin J, Amiot B, Argikar UA, Remmel RP, Rinaldo P. Rapid, large-scale formation of porcine hepatocyte spheroids in a novel spheroid reservoir bioartificial liver. Liver Transpl 2005;11:901-910.
35. Landry J, Bernier D, Ouellet C, Goyette R, Marceau N. Spheroidal aggregate culture of rat liver cells: histotypic reorganization, biomatrix deposition, and maintenance of functional activities. J Cell Biol 1985;101:914-923.
36. Brophy CM, Luebke-Wheeler JL, Amiot BP, Khan H, Remmel RP, Rinaldo P, Nyberg SL. Rat hepatocyte spheroids formed by rocked technique maintain differentiated hepatocyte gene expression and function. Hepatology 2009;49:578-586.
37. Nguyen PK, Riegler J, Wu JC. Stem cell imaging: from bench to bedside. Cell Stem cell 2014;14:431-444.
38. Contag CH, Contag PR, Mullins JI, Spilman SD, Stevenson DK, Benaron DA. Photonic detection of bacterial pathogens in living hosts. Mol Microbiol 1995;18:593-603.
39. Turner RA, Wauthier E, Lozoya O, McClelland R, Bowsher JE, Barbier C, et al. Successful transplantation of human hepatic stem cells with restricted localization to liver using hyaluronan grafts. Hepatology 2013;57: 775-784.
40. Chen IY, Wu JC. Cardiovascular molecular imaging: focus on clinical translation. Circulation 2011;123:425-443.
41. Luker GD, Luker KE. Optical imaging: current applications and future directions. J Nucl Med 2008;49:1-4.
42. Hickey RD, Lillegard JB, Fisher JE, McKenzie TJ, Hofherr SE, Finegold MJ, et al. Efficient production of Fah-null heterozygote pigs by chimeric adeno-associated virus-mediated gene knockout and somatic cell nuclear transfer. Hepatology 2011;54:1351-1359.
43. Hickey RD, Mao SA, Glorioso J, Lillegard JB, Fisher JE, Amiot B, et al. Fumarylacetoacetate hydrolase deficient pigs are a novel large animal model of metabolic liver disease. Stem Cell Res 2014;13:144-153.
44. Rogers CS, Stoltz DA, Meyerholz DK, Ostedgaard LS, Rokhlina T, Taft PJ, et al. Disruption of the CFTR gene produces a model of cystic fibrosis in newborn pigs. Science 2008;321:1837-1841.
45. Gupta S, Lee CD, Vemuru RP, Bhargava KK. 111Indium labeling of hepatocytes for analysis of short-term biodistribution of transplanted cells. Hepatology 1994;19:750-757.
46. Cheng K, Benten D, Bhargava K, Inada M, Joseph B, Palestro C, Gupta S. Hepatic targeting and biodistribution of human fetal liver stem/progenitor cells and adult hepatocytes in mice. Hepatology 2009;50:1194-1203.
47. Defresne F, Tondreau T, Stéphenne X, Smets F, Bourgois A, Najimi M, et al. Biodistribution of adult derived human liver stem cells following intraportal infusion in a 17-year-old patient with glycogenosis type 1A. Nucl Med Biol 2014;41:371-375.
48. Bohnen NI, Charron M, Reyes J, Rubinstein W, Strom SC, Swanson D, Towbin R. Use of indium-111-labeled hepatocytes to determine the biodistribution of

transplanted hepatocytes through portal vein infusion. Clin Nucl Med 2000;25:447-450.

49. Templin C, Zweigerdt R, Schwanke K, Olmer R, Ghadri JR, Emmert MY, et al. Transplantation and tracking of human-induced pluripotent stem cells in a pig model of myocardial infarction: assessment of cell survival, engraftment, and distribution by hybrid single photon emission computed tomography/computed tomography of sodium iodide symporter transgene expression. Circulation 2012;126:430-439.
50. Wangensteen KJ, Wilber A, Keng VW, He Z, Matise I, Wangensteen L, et al. A facile method for somatic, lifelong manipulation of multiple genes in the mouse liver. Hepatology 2008;47:1714-1724.
51. Wilber A, Wangensteen KJ, Chen YX, Zhuo LJ, Frandsen JL, Bell JB, et al. Messenger RNA as a source of transposase for sleeping beauty transposon-mediated correction of hereditary tyrosinemia type I. Mol Ther 2007;15:1280-1287.
52. Moolten FL. Tumor chemosensitivity conferred by inserted herpes thymidine kinase genes: paradigm for a prospective cancer control strategy. Cancer Res 1986;46: 5276-5281.
53. Di Stasi A, Tey SK, Dotti G, Fujita Y, Kennedy-Nasser A, Martinez C, et al. Inducible apoptosis as a safety switch for adoptive cell therapy. N Engl J Med 2011;365:1673-1683.
54. Wilson JM, Johnston DE, Jefferson DM, Mulligan RC. Correction of the genetic defect in hepatocytes from the Watanabe heritable hyperlipidemic rabbit. Proc Natl Acad Sci U S A 1988;85:4421-4425.
55. Matas AJ, Sutherland DE, Steffes MW, Mauer SM, Sowe A, Simmons RL, Najarian JS. Hepatocellular transplantation for metabolic deficiencies: decrease of plasms bilirubin in Gunn rats. Science 1976;192:892-894.
56. Yamanouchi K, Zhou H, Roy-Chowdhury N, Macaluso F, Liu L, Yamamoto T, et al. Hepatic irradiation augments engraftment of donor cells following hepatocyte transplantation. Hepatology 2009;49:258-267.
57. Aiuti A, Biasco L, Scaramuzza S, Ferrua F, Cicalese MP, Baricordi C, et al. Lentiviral hematopoietic stem cell gene therapy in patients with Wiskott-Aldrich syndrome. Science 2013;341:1233151.
58. Biffi A, Montini E, Lorioli L, Cesani M, Fumagalli F, Plati T, et al. Lentiviral hematopoietic stem cell gene therapy benefits metachromatic leukodystrophy. Science 2013; 341:1233158.
59. Wilber A, Wangensteen KJ, Chen Y, Zhuo L, Frandsen JL, Bell JB, et al. Messenger RNA as a source of transposase for sleeping beauty transposon-mediated correction of hereditary tyrosinemia type I. Mol Ther 2007;15:1280-1287.
60. Wu G, Liu N, Rittelmeyer I, Sharma AD, Sgodda M, Zaehres H, et al. Generation of healthy mice from gene-corrected disease-specific induced pluripotent stem cells. PLoS Biol 2011;9:e1001099.
61. Pedraza-Lopez M, Ferro-Flores G, Mendiola-Cruz MT, Morales-Ramirez P. Assessment of radiation-induced DNA damage caused by the incorporation of 99mTc-radiopharmaceuticals in murine lymphocytes using single cell gel electrophoresis. Mutat Res 2000;465:139-144.
62. Smith T, Petoussi-Henss N, Zankl M. Comparison of internal radiation doses estimated by MIRD and voxel techniques for a "family" of phantoms. Eur J Nucl Med 2000;27:1387-1398.
63. American College of Radiology and Radiological Society of North America. Patient safety: radiation dose in x-ray and ct exams. www.radiologyinfo.org/en/safety/index.cfm?pg=sfty_xray. Accessed on August 10, 2014.
64. National Council on Radiation Protection and Measurements. Ionizing radiation exposure of the population of the United States, NCRP Report No. 160. Bethesda, MD: NCRPM; 2009.
65. United Nations Scientific Committee on the Effects of Atomic Radiation. Attributing health effects to radiation exposure and inferring risks. 59th session (suppl 46), 21-25 May 2012. UNSCEAR; 2012. United Nations, New York, NY, USA.